Supplement of Atmos. Chem. Phys., 23, 6395–6407, 2023
https://doi.org/10.5194/acp-23-6395-2023-supplement

Atmospheric Chemistry and Physics
Open Access
EGU

Supplement of

High contribution of anthropogenic combustion sources to atmospheric inorganic reactive nitrogen in South China evidenced by isotopes

Tingting Li et al.

Correspondence to: Jun Li (junli@gig.ac.cn)

Text S1 Chemical components analysis

OC/EC: OC and EC contents were analyzed by thermal-optical carbon analyzer (Sunset Laboratory Inc). One punch of 1.5 cm^2 filter samples was cut and put into the instrument. Blank samples were measured by the same methods. Quality control standards (sucrose solutions) were dropped onto quartz membranes to dry and then the carbon content was tested in the same way to ensure that the instrument was stable before measurement and in the testing process.

Water-soluble ions: Na^+, K^+, Mg^{2+}, Ca^{2+}, NH_4^+, Cl^-, SO_4^{2-}, and NO_3^- were measured by ion chromatography. The blank samples were also analyzed following the same procedure for samples. Reagent blanks (ultrapure water) and quality control standards were measured every 10 samples to detect contamination and drift.

Isotopic analysis: The $\delta^{15}N\text{-}NO_3^-$ and $\delta^{18}O\text{-}NO_3^-$ values (‰) were corrected by multi-point correction (r^2=0.999) based on international standards (IAEA-NO3, USGS32, USGS34, and USGS35) and $\delta^{15}N\text{-}NH_4^+$ was corrected by international standards (IAEA-N1, USGS25, and USGS26) (Sun et al., 2021; Zong et al., 2017).

Radioactive isotope analysis: ^{210}Pb and ^{7}Be were analyzed at Shenzhen University using high-purity γ spectrometer equipped with an HPGe detector (Jiang et al., 2021; Liu et al., 2020). ^{210}Pb in the atmosphere mainly comes from terrestrial sources and is effective indicator of the aerosols transport from the continental surface. The $f(^{7}Be, ^{210}Pb)$ index is powerful to reveal the influence of atmospheric dynamic transport on variations in aerosol pollutants, and expressed as following equation (Jiang et al., 2021). Generally, the relatively high values of $f(^{7}Be, ^{210}Pb)$ index represented that the aerosol pollutants were influenced by long-range transport from the upper air.

$$f(^{7}Be,^{210}Pb) = \frac{[^{7}Be]}{[^{7}Be]+n[^{210}Pb]} \qquad (S1)$$

where $[^{7}Be]$ and $[^{210}Pb]$ are activity concentrations of ^{7}Be and ^{210}Pb, respectively, n is estimated as the ratio of the standard deviation of $[^{7}Be]$ to $[^{210}Pb]$.

Trace gas: concentrations of trace gases (NO, NO_2, SO_2, O_3, and CO) were acquired from online equipment. The online equipment included a gas filter analyzer (Thermo Scientific, Model 48i) to measure CO, a pulse fluorescence analyzer (Thermo

Scientific, Model 43iTLE) to measure SO_2 and O_3, and a chemiluminescence apparatus (Thermo Scientific, Model 42iTL) to measure NO and NO_2.

Meteorological parameters: Temperature, relative humidity, wind speed, and atmospheric pressure were also acquired by a portable weather analyzer (WXT520, Vaisala, Finland). Trace gas concentrations and meteorological parameters were hourly data. In this study, average data of 24 hours through a sampling period were used.

Text S2 Sources of atmospheric NH_3 and NOx in Guangzhou, NO_3^- formation pathways in Guangzhou

Atmospheric NH_3 sources. There are two major groups of atmospheric NH_3 emission sources(Chen et al., 2022b). One is NH_3 volatilization from NH_4^+-containing substrates (mainly fertilized and natural soils, livestock, human wastes, and natural and N-polluted water). Although Guangzhou is an urban site, the emission inventory results showed a high contribution of nitrogen fertilizers application and livestock to atmospheric NH_3 (Zheng et al., 2012), which may be influenced by agricultural activities around Guangzhou. Human waste is also an important contributor to NH_3 in cities, as suggested by a study in Shanghai(Chang et al., 2015). Guangzhou is one of China's megacities with a dense population, so the contribution of human waste to atmospheric NH_3 in Guangzhou cannot be ignored. Therefore, nitrogen fertilizers application, livestock, and human waste were considered as sources of volatilization NH_3 in this study. In addition, the other group is NH_3 associated with combustion sources (such as coal burning, vehicles, and biomass burning). The contribution of biomass burning and coal combustion to NH_3 was very high (about 76.3%) in developing countries, as suggested by the global high-resolution emissions inventory (Meng et al., 2017). NH_3 in Chinese cities was indeed influenced by coal and biomass combustion evidenced by isotopes(Xiao et al., 2020; Liu et al., 2018; Pan et al., 2018). Selective catalytic reduction technology equipped with vehicles and industrial boiler is also an important source of NH_3(Meng et al., 2017). With the rapid increase in vehicle ownership, vehicle emission has a significant impact on urban NH_3, which was confirmed by tunnel tests in Guangzhou (Liu et al., 2014). Therefore, biomass burning,

coal combustion, and vehicles were considered as sources of combustion NH_3 in this study.

Atmospheric NOx sources. We considered coal combustion, mobile traffic sources, biomass burning, and soil microbial activity as dominant atmospheric NOx sources. Based on bottom-up emission inventory, power plant, industry, residential use, and transportation were the traditional NOx emission sources in cities in China, including Guangzhou (Liu et al., 2017a). According to the type of fuel combustion, traditional sources of NOx could be roughly divided into coal combustion (power plant, industry, and residential use) and mobile sources (transportation including vehicle exhaust and ship emission). Furthermore, recent studies show that biomass burning is an essential source of NOx based on emission factor study (Mehmood et al., 2017) and isotopic evidence (Zong et al., 2020). Microbial process emission is another important source of NOx, in which nitrification or denitrification microbial bacteria widely distributed in soils consume accumulated nitrogen and release NO as a byproduct(Hall and Matson, 1996; Jaeglé et al., 2004). The cultivated land with extensive use of nitrogen fertilizer in the suburbs around Guangzhou is also an important source of NOx, which is named as microbial process in this study. δ^{15}N-NOx values differed significantly among these four sources, which allows us to differentiate their relative contributions to the mixture of atmospheric. We did not consider NO_3^- from lightning because it accounts for less than 5% of global terrestrial NOx emissions(Song et al., 2021; Qu et al., 2020; Pickering et al., 2016).

NO_3^- formation pathways. There are several major formation pathways of NO_3^-.

P1 (NO_2+·OH), NO_2 is oxidized by ·OH to form HNO_3, then reacts with alkaline substances (such as NH_3) to form NO_3^-.

P2 (N_2O_5), NO_2 is oxidized by O_3 to form ·NO_3, ·NO_3 reacts with NO_2 to form N_2O_5, then the hydrolysis of N_2O_5 on aerosol surfaces produces NO_3^-.

P3 (·NO_3+org), the NO_2 is oxidized by O_3 to form ·NO_3, then the ·NO_3 reacts with organic, such as dimethyl sulfide (DMS) or hydrocarbons (HC) to form HNO_3, and then NO_3^-.

P4(·NO_3+·HO_2), NO_2 is oxidized by O_3 to form ·NO_3, ·NO_3 reacts with ·HO_2 to

form HNO_3.

The P1 (·OH) and P2 (N_2O_5) pathways are dominant formation pathways. Song reported that ·OH and N_2O_5 pathways contributed 43% and 32% to NO_3^-, respectively, by isotope tracing (Song et al., 2021). Based on isotopic estimates, the contribution of ·NO3+org to NO_3^- was relatively high, e.g., about 16% in Beijing(Song et al., 2021). However, the proportion of $\cdot NO_3$+org estimated by the Community Multiscale Air Quality (CAMQ) model was very low in the YRD(Sun et al., 2022) and PRD(Qu et al., 2021), especially in Guangzhou (central PRD) where it is only 4%(Qu et al., 2021). The ·OH and N_2O_5 were the dominant pathways and contributed 94% to NO_3^- in Guangzhou (Qu et al., 2021). We speculate that the different contribution of $\cdot NO_3$+org pathway between Guangzhou and Beijing may be caused by the difference in atmospheric oxidation. The ozone pollution is serious in Guangzhou due to a unique synoptic system including the surface high-pressure system, hurricane movement, and sea–land breeze(Tan et al., 2019). And the atmospheric ·OH reactivity in Guangzhou was higher than in several cities, including Beijing (Tan et al., 2019). Take DMS as an example, the main oxidant of DMS is ·OH (Andreae and Crutzen, 1997). However, in the cold season or remote regions, the $\cdot NO_3$ radical can also play an important role in reaction with DMS (addition reaction and hydrogen abstraction) (Andreae and Crutzen, 1997; Yin et al., 1990). The high reactivity of ·OH may reduce the contribution of $\cdot NO_3$ to DMS in Guangzhou due to the competition between ·OH and $\cdot NO_3$ to react with DMS. Therefore, the contribution of $\cdot NO_3$+org to NO_3^- was relatively low. In addition, the $\delta^{18}O$ of NO_3^- formed by the N_2O_5 and $\cdot NO_3$+org pathway is similar(Walters and Michalski, 2016). The introduction of the $\cdot NO_3$+org pathway would greatly increase the uncertainty of the contribution of N_2O_5 pathways. While the $\delta^{18}O$ of NO_3^- formed by the ·OH and N_2O_5 pathway differ significantly, which allows to differentiate their relative contributions to NO_3^-. Therefore, we considered only the ·OH and N_2O_5 pathways in this study.

Specifically, the ·OH and N_2O_5 pathways are expressed by R1-R8. Once emitted into the atmosphere, NOx is oxidized to HNO_3 or NO_3^- via the following chemical pathways (R1-R8) (Fang et al., 2011). In summary, NOx oxygen atoms are rapidly

exchanged with O_3 in the NO/NO_2 cycle (R1-R3); ·OH radicals result in the oxidation of NO_2 to HNO_3 (R4; the ·OH pathway); NO_2 is oxidized by O_3 to produce ·NO_3 (R5), which subsequently combines with NO_2 to form N_2O_5 (R6), and then undergoes hydrolysis to form HNO_3 (R7), referred to as the O_3 pathway; and the generated HNO_3 combines with alkali to form NO_3^- (R8). Overall, the ·OH and O_3 pathways are the two fundamental oxidation pathways for NOx, generally exhibiting noticeable diurnal and seasonal variation(Elliott et al., 2007). Previous research has found that the ·OH pathway is more prevalent during the daytime and in summer when the relative concentration of ·OH is higher. Conversely, the O_3 pathway is more dominant overnight and in winter, because N_2O_5 is thermally unstable(Hastings et al., 2003; Xiao et al., 2015). The O_3 in the troposphere has a higher $\delta^{18}O$ value, while $\delta^{18}O$-OH and $\delta^{18}O$-H_2O is lower. The $\delta^{18}O$-HNO_3 formed by the ·OH pathway is contributed by 2/3 O_3 and 1/3 ·OH (R4), while in the N_2O_5 hydrolysis pathway after oxidation by O_3, the $\delta^{18}O$-HNO_3 is contributed by 5/6 O_3 and 1/6 H_2O (R5-R7). Therefore, the $\delta^{18}O$-NO_3^- formed through the ·OH pathway is lower than the N_2O_5 pathway.

$$NO + O_3 \rightarrow NO_2 + O_2 \quad (R1)$$

$$NO_2 + hv \rightarrow NO + O \quad (R2)$$

$$O + O_2 \rightarrow O_3 \quad (R3)$$

$$NO_2 + \cdot OH \rightarrow HNO_3 \quad (R4)$$

$$NO_2 + O_3 \rightarrow NO_3 + O_2 \quad (R5)$$

$$NO_2 + NO_3 \rightarrow N_2O_5 \quad (R6)$$

$$N_2O_5 + H_2O \rightarrow 2HNO_3 \quad (R7)$$

$$HNO_3 + Alkali \rightarrow NO_3^- \quad (R8)$$

Text S3 The estimation of $\delta^{15}N$-NH_4^+ from sugarcane leaf burning

The $\delta^{15}N$ in sugarcane leaf is 38‰ (Martinellia et al., 2002), which may consist of N-NO_X and N-NH_3. The $\delta^{15}N$-NOx from biomass burning is 1.04‰(Zong et al., 2017). According to the assumption of different proportions (from 5% to 95%) of N-NO_X and N-NH_3 from sugarcane leaf, shown in **Table S2**. The mean value among the proportion (from 5% to 95%) of N-NH_4^+ in sugarcane leaf was 37.48‰. In addition, the $\delta^{15}N$ of

particulate matters from biomass burning was 6.6‰ higher than that of biomass (Martinellia et al., 2002). Therefore, $\delta^{15}N\text{-}NH_4^+$ from sugarcane leaf burning may be 44.08‰.

Figure S1-Figure S6

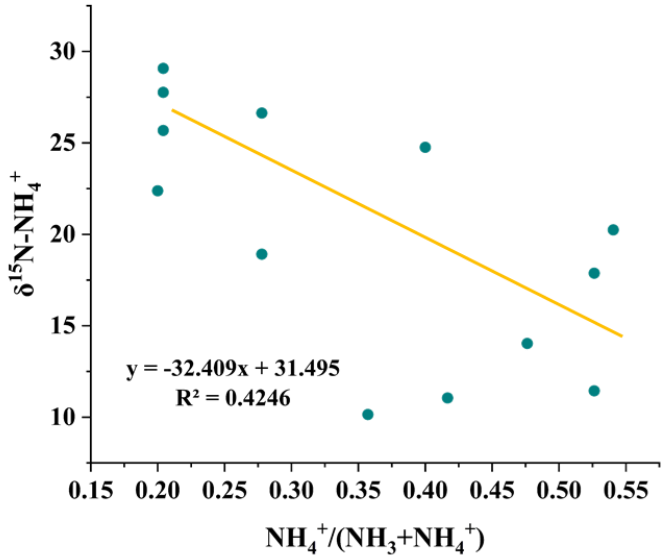

Figure S1. Linear fitting of $NH_4^+/(NH_3+NH_4^+)$ with $\delta^{15}N\text{-}NH_4^+$.

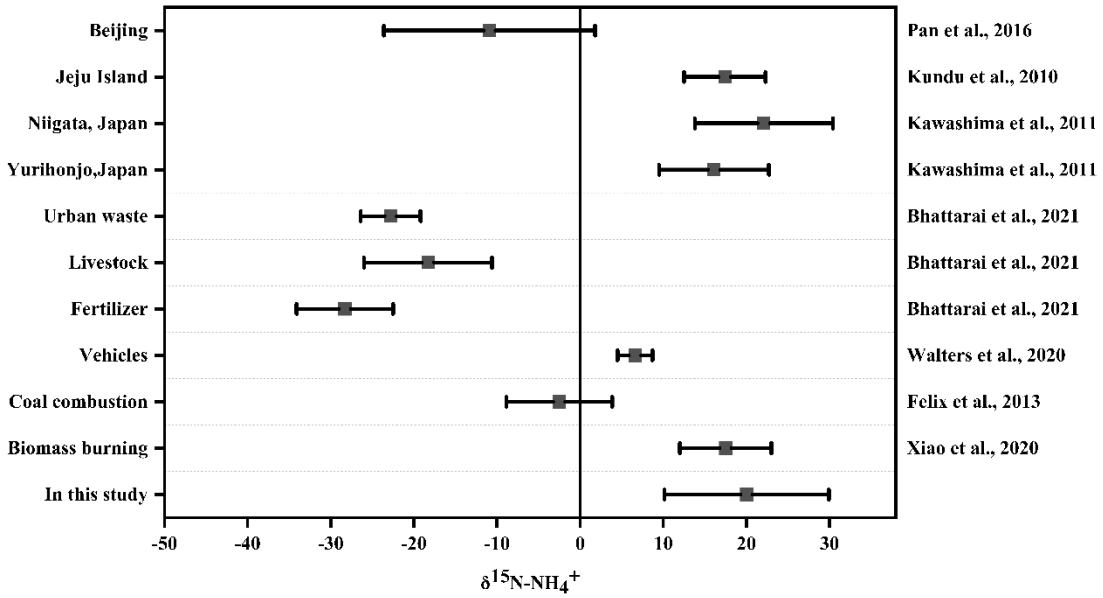

Figure S2. Ranges of $\delta^{15}N\text{-}NH_4^+$ from different sites(Pan et al., 2016; Kundu et al., 2010; Kawashima and Kurahashi, 2011) and different emission sources(Felix et al., 2013; Bhattarai et al., 2021; Chang et al., 2016; Xiao et al., 2020).

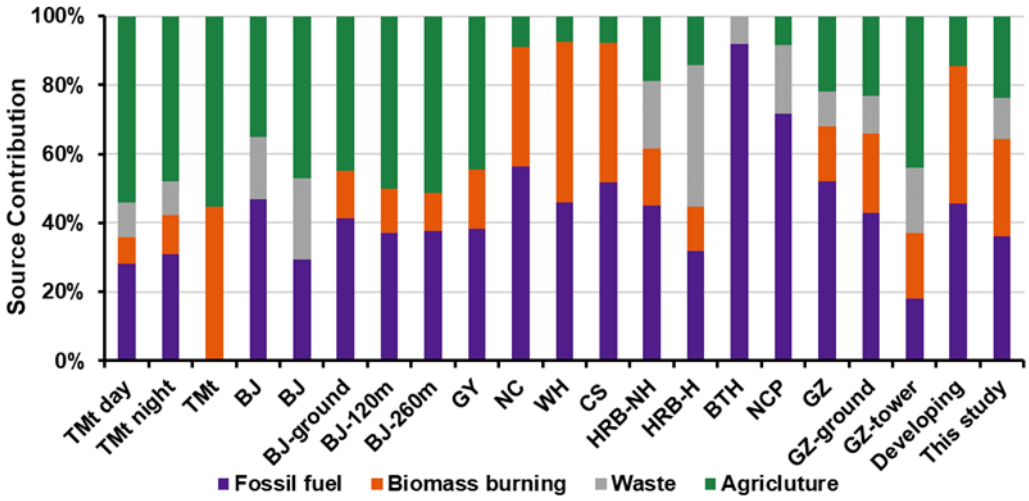

Figure S3. The comparison of sources apportionment results of atmospheric NH_3 and NH_4^+ in different sites in China. Background site in Tai mountain[TMt] (Wu et al., 2021; Chang et al., 2019), urban sites in North China (Beijing [BJ] (Pan et al., 2020; Chang et al., 2016), vertical profile observation in Beijing (ground, 120m height, and 260m height [BJ-ground, BJ-120m, and BJ-260m] (Wu et al., 2019), Jingjinji region [BTH] (Zhang et al., 2020), and North China plain [NCP]) (Xiang et al., 2022), East North China (Harbin heating period and non-heating period [HRB-H and HRB-NH]) (Sun et al., 2021), Central China (Wuhan [WH] and Changsha [CS]) (Xiao et al., 2020), East China (Nangchang [NC]) (Xiao et al., 2020), Southwest China (Guiyang [GY], source in precipitation) (Liu et al., 2017b), and South China (Guangzhou[GZ]) (Liu et al., 2018), vertical profile observation in Guangzhou(ground and Guangzhou tower [GZ-ground and GZ-tower])(Chen et al., 2022a). Source of NH_3 were estimated by inventory methods in developing country[developing] (Meng et al., 2017).

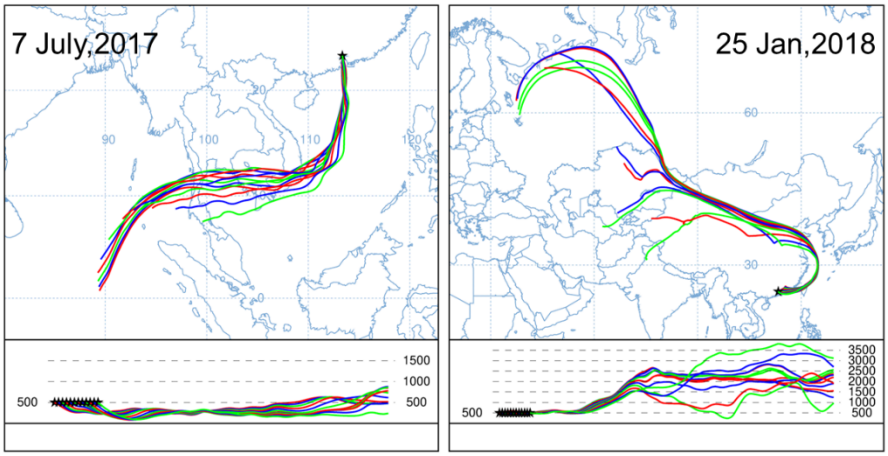

Figure S4. The air mass backward trajectory to receptor site on 7 July,2017 and 25 Jan,2018.

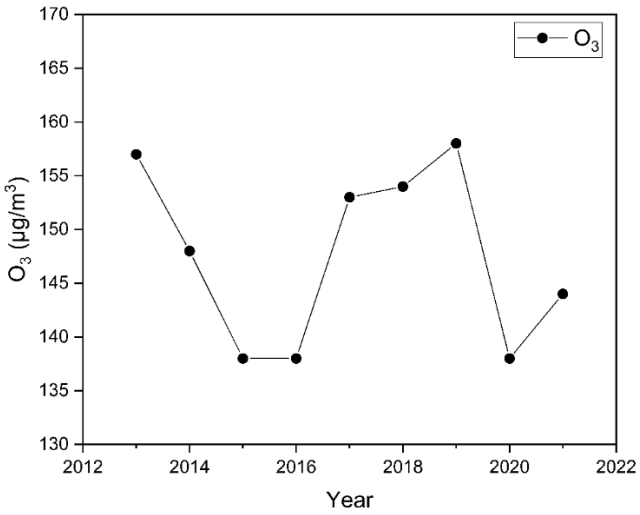

Figure S5. The temporal variation of O_3 concentration in PRD from 2013 to 2021.

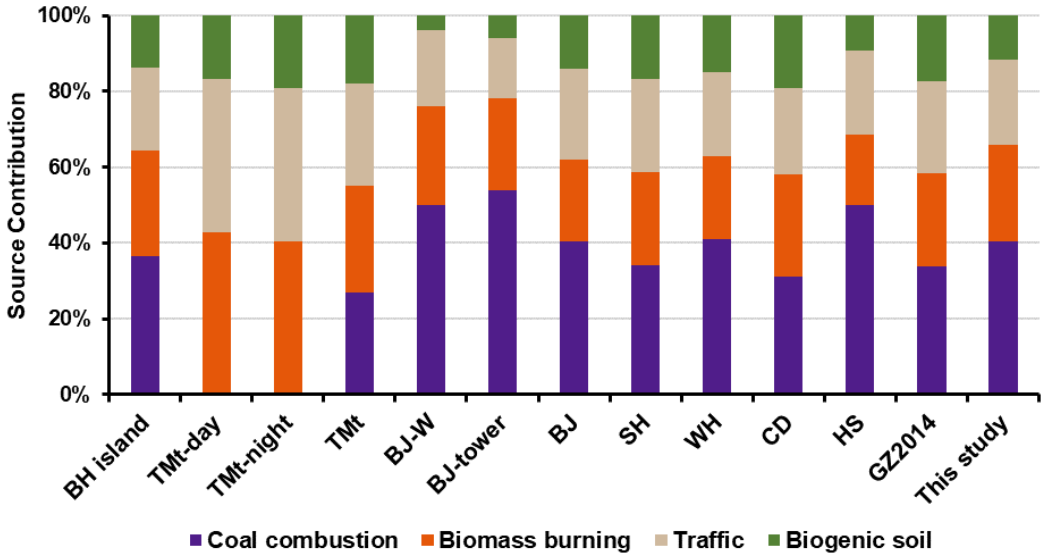

Figure S6. The comparison of sources apportionment results of atmospheric NOx and NO_3^- in different sites in China. Background in Beihuangcheng island [BH island](Zong et al., 2017) and Tai mountain [TMt] (Wu et al., 2021), urban sites in North China (Beijing [BJ] (Zong et al., 2020), Beijing winter [BJ-W] (Fan et al., 2020), and vertical profile observation in Beijing [BJ-tower](Fan et al., 2022)), Central China (Wuhan [WH]) (Zong et al., 2020), East China (Shanghai [SH]) (Zong et al., 2020), Southwest China (Chengdu [CD]), and South China (Guangzhou [GZ2014] and Heshan [HS])(Zong et al., 2020; Su et al., 2020).

Table S1-Table S2

Table S1. Test constants of A, B, C, and D over the settled temperature range of 150−450K(Zong et al., 2017; Walters and Michalski, 2016; Walters et al., 2016; Walters and Michalski, 2015).

$^{m}\alpha_{X/Y}$	A	B	C	D
$^{15}NO_2/NO$	3.8834	-7.7299	6.0101	-0.17928
$^{15}N_2O_5/NO_2$	0.69398	-1.9859	2.3876	0.16308
$^{18}NO/NO_2$	-0.04129	1.1605	-1.8829	0.74723
$^{18}H_2O/OH$	2.1137	-3.8026	2.5653	0.59410

Table S2. The estimation of $\delta^{15}N\text{-}NH_3$ in sugarcane leaf.

N-NOx in sugarcane leaf (%)	5	25	50	75	95
$\delta^{15}N$ in sugarcane leaf (‰)	38	38	38	38	38
$\delta^{15}N\text{-}NOx$ (‰)	1.04	1.04	1.04	1.04	1.04
Caculated results $\delta^{15}N\text{-}NH_3$ (‰)	37.95	37.74	37.48	37.22	37.01

References:

Andreae, M. O. and Crutzen, P. J.: Atmospheric aerosols: biogeochemical sources and role in atmospheric chemistry, Science, 276, 1052-1058, https://doi.org/10.1126/science.276.5315.1052, 1997.

Bhattarai, N., Wang, S., Pan, Y., Xu, Q., Zhang, Y., Chang, Y., and Fang, Y.: $\delta^{15}N$-stable isotope analysis of NHx : An overview on analytical measurements, source sampling and its source apportionment, Front. Environ. Sci. Eng., 15, 126, https://doi.org/10.1007/s11783-021-1414-6, 2021.

Chang, Y., Deng, C., Dore, A. J., and Zhuang, G.: Human Excreta as a Stable and Important Source of Atmospheric Ammonia in the Megacity of Shanghai, PLoS One, 10, e0144661, https://doi.org/10.1371/journal.pone.0144661, 2015.

Chang, Y., Liu, X., Deng, C., Dore, A. J., and Zhuang, G.: Source apportionment of atmospheric ammonia before, during, and after the 2014 APEC summit in Beijing using stable nitrogen isotope signatures, Atmos. Chem. Phys., 16, 11635-11647, https://doi.org/10.5194/acp-16-11635-2016, 2016.

Chang, Y., Zhang, Y.-L., Li, J., Tian, C., Song, L., Zhai, X., Zhang, W., Huang, T., Lin, Y.-C., Zhu, C., Fang, Y., Lehmann, M. F., and Chen, J.: Isotopic constraints on the atmospheric sources and formation of nitrogenous species in clouds influenced by biomass burning, Atmos. Chem. Phys., 19, 12221–12234, https://doi.org/10.5194/acp-19-12221-2019, 2019.

Chen, Z., Pei, C., Liu, J., Zhang, X., Ding, P., Dang, L., Zong, Z., Jiang, F., Wu, L., Sun, X., Zhou, S., Zhang, Y., Zhang, Z., Zheng, J., Tian, C., Li, J., and Zhang, G.: Non-agricultural source dominates the ammonium aerosol in the largest city of South China based on the vertical $\delta^{15}N$ measurements,

Sci. Total Environ., 848, 157750, https://doi.org/10.1016/j.scitotenv.2022.157750, 2022a.

Chen, Z. L., Song, W., Hu, C. C., Liu, X. J., Chen, G. Y., Walters, W. W., Michalski, G., Liu, C. Q., Fowler, D., and Liu, X. Y.: Significant contributions of combustion-related sources to ammonia emissions, Nat. Commun., 13, 7710, https://doi.org/10.1038/s41467-022-35381-4, 2022b.

Elliott, E. M., Kendall, C., Wankel, S. D., Burns, D. A., Boyer, E. W., Harlin, K., Bain, D. J., and Butler, T. J.: Nitrogen isotopes as indicators of NOx source contributions to atmospheric nitrate deposition across the midwestern and Northeastern United States, Environ. Sci. Technol., 41, 7661-7667, https://doi.org/10.1021/es070898t, 2007.

Fan, M.-Y., Zhang, Y.-L., Hong, Y., Lin, Y.-C., Zhao, Z.-Y., Cao, F., Sun, Y., Guo, H., and Fu, P.: Vertical differences of nitrate sources in urban boundary layer based on tower measurements, Environ. Sci. Technol. Lett., 2c00600, https://doi.org/10.1021/acs.estlett.2c00600, 2022.

Fan, M. Y., Zhang, Y. L., Lin, Y. C., Cao, F., Zhao, Z. Y., Sun, Y., Qiu, Y., Fu, P., and Wang, Y.: Changes of emission sources to nitrate aerosols in Beijing after the clean air actions: evidence from dual isotope compositions, J. Geophys. Res.: Atmos., 125, 031998, https://doi.org/10.1029/2019jd031998, 2020.

Fang, Y. T., Koba, K., Wang, X. M., Wen, D. Z., Li, J., Takebayashi, Y., Liu, X. Y., and Yoh, M.: Anthropogenic imprints on nitrogen and oxygen isotopic composition of precipitation nitrate in a nitrogen-polluted city in southern China, Atmos. Chem. Phys., 11, 1313-1325, https://doi.org/10.5194/acp-11-1313-2011, 2011.

Felix, J. D., Elliott, E. M., Gish, T. J., McConnell, L. L., and Shaw, S. L.: Characterizing the isotopic composition of atmospheric ammonia emission sources using passive samplers and a combined oxidation-bacterial denitrifier approach, Rapid Commun. Mass Spectrom., 27, 2239-2246, https://doi.org/10.1002/rcm.6679, 2013.

Hall, S. J. and Matson, P. A.: NOx emissions from soil: implications for air quality modeling in agricultural regions, Annu. Rev. Energy Environ., 21, 311-346, https://doi.org/10.1146/annurev.energy.21.1.311, 1996.

Hastings, M. G., Sigman, D. M., and Lipschultz, F.: Isotopic evidence for source changes of nitrate in rain at Bermuda, J. Geophys. Res.: Atmos., 108, 1-12, https://doi.org/10.1029/2003jd003789, 2003.

Jaeglé, L., Martin, R. V., Chance, K., Steinberger, L., Kurosu, T. P., Jacob, D. J., Modi, A. I., Yoboué, V., Sigha-Nkamdjou, L., and Galy-Lacaux, C.: Satellite mapping of rain-induced nitric oxide emissions from soils, J. Geophys. Res.: Atmos., 109, D21310, https://doi.org/10.1029/2004jd004787, 2004.

Jiang, H., Li, J., Sun, R., Liu, G., Tian, C., Tang, J., Cheng, Z., Zhu, S., Zhong, G., Ding, X., and Zhang, G.: Determining the sources and transport of brown carbon using radionuclide tracers and modeling, J. Geophys. Res.: Atmos., 126, e2021JD034616, https://doi.org/10.1029/2021jd034616, 2021.

Kawashima, H. and Kurahashi, T.: Inorganic ion and nitrogen isotopic compositions of atmospheric aerosols at Yurihonjo, Japan: implications for nitrogen sources, Atmos. Environ., 45, 6309-6316, https://doi.org/10.1016/j.atmosenv.2011.08.057, 2011.

Kundu, S., Kawamura, K., and Lee, M.: Seasonal variation of the concentrations of nitrogenous species and their nitrogen isotopic ratios in aerosols at Gosan, Jeju Island: Implications for atmospheric processing and source changes of aerosols, J. Geophys. Res. , 115, https://doi.org/10.1029/2009jd013323, 2010.

Liu, F., Beirle, S., Zhang, Q., van der, A. R., Zheng, B., Tong, D., and He, K.: NOx emission trends over Chinese cities estimated from OMI observations during 2005 to 2015, Atmos. Chem. Phys., 17, 9261-9275, https://doi.org/10.5194/acp-17-9261-2017, 2017a.

Liu, G., Wu, J., Li, Y., Su, L., and Ding, M.: Temporal variations of ^{7}Be and ^{210}Pb activity concentrations in the atmosphere and aerosol deposition velocity in Shenzhen, South China, Aerosol Air Qual. Res., 20, 1607–1617, https://doi.org/10.4209/aaqr.2019.11.0560, 2020.

Liu, J., Ding, P., Zong, Z., Li, J., Tian, C., Chen, W., Chang, M., Salazar, G., Shen, C., Cheng, Z., Chen, Y., Wang, X., Szidat, S., and Zhang, G.: Evidence of rural and suburban sources of urban haze formation in China: a case study from the Pearl River Delta region, J. Geophys. Res.: Atmos., 123, 4712-4726, https://doi.org/10.1029/2017jd027952, 2018.

Liu, T., Wang, X., Wang, B., Ding, X., Deng, W., Lü, S., and Zhang, Y.: Emission factor of ammonia (NH_3) from on-road vehicles in China: tunnel tests in urban Guangzhou, Environ. Res. Lett., 9, 064027, https://doi.org/10.1088/1748-9326/9/6/064027, 2014.

Liu, X. Y., Xiao, H. W., Xiao, H. Y., Song, W., Sun, X. C., Zheng, X. D., Liu, C. Q., and Koba, K.: Stable isotope analyses of precipitation nitrogen sources in Guiyang, southwestern China, Environ. Pollut., 230, 486-494, https://doi.org/10.1016/j.envpol.2017.06.010, 2017b.

Martinellia, L. A., Camargoa, P. B., Laraa, L. B. L. S., Victoriaa, R. L., and Artaxo, P.: Stable carbon and nitrogen isotopic composition of bulk aerosol particles in a C4 plant landscape of southeast Brazil, Atmos. Environ., 36, 2427–2432, https://doi.org/10.1016/S1352-2310(01)00454-X, 2002.

Mehmood, K., Chang, S., Yu, S., Wang, L., Li, P., Li, Z., Liu, W., Rosenfeld, D., and Seinfeld, J. H.: Spatial and temporal distributions of air pollutant emissions from open crop straw and biomass burnings in China from 2002 to 2016, Environ. Chem. Lett., 16, 301-309, https://doi.org/10.1007/s10311-017-0675-6, 2017.

Meng, W., Zhong, Q., Yun, X., Zhu, X., Huang, T., Shen, H., Chen, Y., Chen, H., Zhou, F., Liu, J., Wang, X., Zeng, E. Y., and Tao, S.: Improvement of a global high-resolution ammonia emission inventory for combustion and industrial sources with new data from the residential and transportation sectors, Environ. Sci. Technol., 51, 2821-2829, https://doi.org/10.1021/acs.est.6b03694, 2017.

Pan, Y., Tian, S., Liu, D., Fang, Y., Zhu, X., Zhang, Q., Zheng, B., Michalski, G., and Wang, Y.: Fossil fuel combustion-related emissions dominate atmospheric ammonia sources during severe haze episodes: evidence from ^{15}N-stable isotope in size-resolved aerosol ammonium, Environ. Sci. Technol., 50, 8049-8056, https://doi.org/10.1021/acs.est.6b00634, 2016.

Pan, Y., Tian, S., Liu, D., Fang, Y., Zhu, X., Gao, M., Wentworth, G. R., Michalski, G., Huang, X., and Wang, Y.: Source Apportionment of Aerosol Ammonium in an Ammonia-Rich Atmosphere: An Isotopic Study of Summer Clean and Hazy Days in Urban Beijing, J. Geophys. Res.: Atmos., 123, 5681-5689, https://doi.org/10.1029/2017jd028095, 2018.

Pan, Y., Gu, M., He, Y., Wu, D., Liu, C., Song, L., Tian, S., Lü, X., Sun, Y., Song, T., Walters, W. W., Liu, X., Martin, N. A., Zhang, Q., Fang, Y., Ferracci, V., and Wang, Y.: Revisiting the concentration observations and source apportionment of atmospheric ammonia, Adv. Atmos. Sci., 37, 933-938, https://doi.org/10.1007/s00376-020-2111-2, 2020.

Pickering, K. E., Bucsela, E., Allen, D., Ring, A., Holzworth, R., and Krotkov, N.: Estimates of lightning NOx production based on OMI NO_2 observations over the Gulf of Mexico, J. Geophys. Res.: Atmos., 121, 8668-8691, https://doi.org/10.1002/2015jd024179, 2016.

Qu, K., Wang, X., Xiao, T., Shen, J., Lin, T., Chen, D., He, L. Y., Huang, X. F., Zeng, L., Lu, K., Ou, Y., and Zhang, Y.: Cross-regional transport of $PM_{2.5}$ nitrate in the Pearl River Delta, China: Contributions and mechanisms, Sci. Total Environ., 753, 142439, https://doi.org/10.1016/j.scitotenv.2020.142439, 2021.

Qu, Z., Henze, D. K., Cooper, O. R., and Neu, J. L.: Impacts of global NOx inversions on NO_2 and ozone

simulations, Atmos. Chem. Phys., 20, 13109-13130, https://doi.org/10.5194/acp-20-13109-2020, 2020.

Song, W., Liu, X. Y., and Liu, C. Q.: New Constraints on Isotopic Effects and Major Sources of Nitrate in Atmospheric Particulates by Combining $\delta^{15}N$ and $\Delta^{17}O$ Signatures, J. Geophys. Res.: Atmos., 126, https://doi.org/10.1029/2020jd034168, 2021.

Su, T., Li, J., Tian, C., Zong, Z., Chen, D., and Zhang, G.: Source and formation of fine particulate nitrate in South China: Constrained by isotopic modeling and online trace gas analysis, Atmos. Environ., 231, https://doi.org/10.1016/j.atmosenv.2020.117563, 2020.

Sun, J., Qin, M., Xie, X., Fu, W., Qin, Y., Sheng, L., Li, L., Li, J., Sulaymon, I. D., Jiang, L., Huang, L., Yu, X., and Hu, J.: Seasonal modeling analysis of nitrate formation pathways in Yangtze River Delta region, China, Atmos. Chem. Phys., 22, 12629-12646, https://doi.org/10.5194/acp-22-12629-2022, 2022.

Sun, X., Zong, Z., Li, Q., Shi, X., Wang, K., Lu, L., Li, B., Qi, H., and Tian, C.: Assessing the emission sources and reduction potential of atmospheric ammonia at an urban site in Northeast China, Environ. Res., 198, 111230, https://doi.org/10.1016/j.envres.2021.111230, 2021.

Tan, Z., Lu, K., Jiang, M., Su, R., Wang, H., Lou, S., Fu, Q., Zhai, C., Tan, Q., Yue, D., Chen, D., Wang, Z., Xie, S., Zeng, L., and Zhang, Y.: Daytime atmospheric oxidation capacity in four Chinese megacities during the photochemically polluted season: a case study based on box model simulation, Atmos. Chem. Phys., 19, 3493–3513, https://doi.org/10.5194/acp-19-3493-2019, 2019.

Walters, W. W. and Michalski, G.: Theoretical calculation of nitrogen isotope equilibrium exchange fractionation factors for various NOy molecules, Geochim. Cosmochim. Ac., 164, 284-297, https://doi.org/10.1016/j.gca.2015.05.029, 2015.

Walters, W. W. and Michalski, G.: Theoretical calculation of oxygen equilibrium isotope fractionation factors involving various NOy molecules, OH, and H_2O and its implications for isotope variations in atmospheric nitrate, Geochim. Cosmochim. Ac., 191, 89–101 https://doi.org/10.1016/j.gca.2016.06.039, 2016.

Walters, W. W., Simonini, D. S., and Michalski, G.: Nitrogen isotope exchange between NO and NO_2 and its implications for $\delta^{15}N$ variations in tropospheric NOx and atmospheric nitrate, Geophys. Res. Lett., 43, 440-448, https://doi.org/10.1002/2015gl066438, 2016.

Wu, L., Yue, S., Shi, Z., Hu, W., Chen, J., Ren, H., Deng, J., Ren, L., Fang, Y., Li, W., Harrison, R. M., and Fu, P.: Source forensics of inorganic and organic nitrogen using δ15N for tropospheric aerosols over Mt. Tai, npj Clim. Atmos. Sci., 8, https://doi.org/10.1038/s41612-021-00163-0, 2021.

Wu, L., Ren, H., Wang, P., Chen, J., Fang, Y., Hu, W., Ren, L., Deng, J., Song, Y., Li, J., Sun, Y., Wang, Z., Liu, C.-Q., Ying, Q., and Fu, P.: Aerosol ammonium in the urban boundary layer in Beijing: insights from nitrogen isotope ratios and simulations in summer 2015, Environ. Sci. Technol. Lett., 6, 389-395, https://doi.org/10.1021/acs.estlett.9b00328, 2019.

Xiang, Y.-K., Dao, X., Gao, M., Lin, Y.-C., Cao, F., Yang, X.-Y., and Zhang, Y.-L.: Nitrogen isotope characteristics and source apportionment of atmospheric ammonium in urban cities during a haze event in Northern China Plain, Atmos. Environ., 269, 118800, https://doi.org/10.1016/j.atmosenv.2021.118800, 2022.

Xiao, H.-W., Xie, L.-H., Long, A.-M., Ye, F., Pan, Y.-P., Li, D.-N., Long, Z.-H., Chen, L., Xiao, H.-Y., and Liu, C.-Q.: Use of isotopic compositions of nitrate in TSP to identify sources and chemistry in South China Sea, Atmos. Environ., 109, 70-78, https://doi.org/10.1016/j.atmosenv.2015.03.006, 2015.

Xiao, H. W., Wu, J. F., Luo, L., Liu, C., Xie, Y. J., and Xiao, H. Y.: Enhanced biomass burning as a source of aerosol ammonium over cities in central China in autumn, Environ. Pollut., 266, 115278, https://doi.org/10.1016/j.envpol.2020.115278, 2020.

Yin, F., Grosjean, D., and Seinfeld, J. H.: Photooxidation of Dimethyl Sulfide and Dimethyl Disulfide. I: Mechanism Development, J. Atmos. Chem., 11, 309-364, 1990.

Zhang, Z., Zeng, Y., Zheng, N., Luo, L., Xiao, H., and Xiao, H.: Fossil fuel-related emissions were the major source of NH_3 pollution in urban cities of northern China in the autumn of 2017, Environ. Pollut., 256, 113428, https://doi.org/10.1016/j.envpol.2019.113428, 2020.

Zheng, J. Y., Yin, S. S., Kang, D. W., Che, W. W., and Zhong, L. J.: Development and uncertainty analysis of a high-resolution NH_3 emissions inventory and its implications with precipitation over the Pearl River Delta region, China, Atmos. Chem. Phys., 12, 7041-7058, https://doi.org/10.5194/acp-12-7041-2012, 2012.

Zong, Z., Tan, Y., Wang, X., Tian, C., Li, J., Fang, Y., Chen, Y., Cui, S., and Zhang, G.: Dual-modelling-based source apportionment of NOx in five Chinese megacities: providing the isotopic footprint from 2013 to 2014, Environ. Int., 137, 105592, https://doi.org/10.1016/j.envint.2020.105592, 2020.

Zong, Z., Wang, X., Tian, C., Chen, Y., Fang, Y., Zhang, F., Li, C., Sun, J., Li, J., and Zhang, G.: First assessment of NOx sources at a regional background site in North China using isotopic analysis linked with modeling, Environ. Sci. Technol., 51, 5923-5931, https://doi.org/10.1021/acs.est.6b06316, 2017.